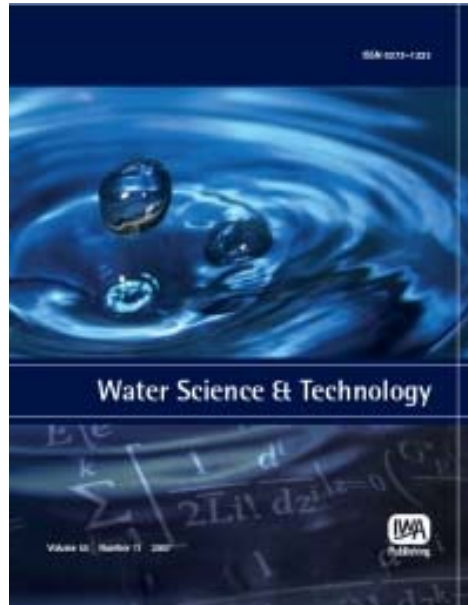


**Provided for non-commercial research and educational use only.
Not for reproduction or distribution or commercial use.**



This article was originally published by IWA Publishing. IWA Publishing recognizes the retention of the right by the author(s) to photocopy or make single electronic copies of the paper for their own personal use, including for their own classroom use, or the personal use of colleagues, provided the copies are not offered for sale and are not distributed in a systematic way outside of their employing institution.

Please note that you are not permitted to post the IWA Publishing PDF version of your paper on your own website or your institution's website or repository.

Please direct any queries regarding use or permissions to wst@iwap.co.uk

Comparative study on adsorption of perfluorooctane sulfonate (PFOS) and perfluorooctanoate (PFOA) by different adsorbents in water

Yuan Yao, Konstantin Volchek, Carl E. Brown, Adam Robinson and Terry Obal

ABSTRACT

Perfluorinated compounds (PFCs) are emerging environmental pollutants. Perfluorooctane sulfonate (PFOS) and perfluorooctanoate (PFOA) are the two primary PFC contaminants that are widely found in water, particularly in groundwater. This study compared the adsorption behaviors of PFOS and PFOA on several commercially available adsorbents in water. The tested adsorbents include granular activated carbon (GAC: Filtrasorb 400), powdered activated carbon, multi-walled carbon nanotube (MCN), double-walled carbon nanotube, anion-exchange resin (AER: IRA67), non-ion-exchange polymer, alumina, and silica. The study demonstrated that adsorption is an effective technique for the removal of PFOS/PFOA from aqueous solutions. The kinetic tests showed that the adsorption onto AER reaches equilibrium rapidly (2 h), while it takes approximately 4 and 24 h to reach equilibrium for MCN and GAC, respectively. In terms of adsorption capacity, AER and GAC were identified as the most effective adsorbents to remove PFOS/PFOA from water. Furthermore, MCN, AER, and GAC proved to have high PFOS/PFOA removal efficiencies ($\geq 98\%$). AER (IRA67) and GAC (Filtrasorb 400) were thus identified as the most promising adsorbents for treating PFOS/PFOA-contaminated groundwater at mg L^{-1} level based on their equilibrium times, adsorption capacities, removal efficiencies, and associated costs.

Key words | adsorption, isotherm, kinetics, PFOA, PFOS, removal efficiency

Yuan Yao (corresponding author)
Konstantin Volchek
Carl E. Brown
Emergencies Science and Technology,
Environment Canada,
335 River Road,
Ottawa,
ON K1A 0H3,
Canada
E-mail: yuan.yao@ec.gc.ca

Adam Robinson
Terry Obal
Maxxam Analytics,
6740 Campobello Road,
Mississauga,
ON L5N 2L8,
Canada

INTRODUCTION

Perfluorinated compounds (PFCs) are a class of anthropogenic organofluorine compounds, which consist of carbon chains saturated with fluorine atoms. PFCs have been synthesized since the 1960s. Due to their excellent thermal stability and hydrophobic properties, PFCs have a wide variety of applications such as non-stick polymers, water- and stain-proof coatings for paper and textiles, oxidation protective coatings on metals, inert surfactants for semiconductor etching, thermally stable lubricants, and aqueous film forming foams (AFFFs) (Vecitis *et al.* 2009). On the other hand, due to their unique physicochemical properties, PFCs have been found to be environmentally persistent and bioaccumulative. Perfluorooctane sulfonate (PFOS) and perfluorooctanoate (PFOA), the two primary PFC contaminants in particular, have been detected globally in the hydrosphere, atmosphere, and biosphere. PFOS was categorized as a persistent organic

pollutant under the Stockholm Convention in May 2009, due to its high persistence, bioaccumulation, long-range transport potential, and toxic effects.

As a result of its high water solubility, PFOS can easily migrate in water environments. It has been detected in rivers, lakes, wastewater, groundwater, and even tap water at concentrations ranging from non-detectable to ng L^{-1} levels throughout the world (Hansen *et al.* 2002; So *et al.* 2004; Fujii *et al.* 2007; Becker *et al.* 2008; Lien *et al.* 2008; Murakami *et al.* 2009). In addition, PFOS concentrations at mg L^{-1} level were detected in groundwater collected from US military bases where AFFFs were used for fire-fighting activities (Schultz *et al.* 2004) as well as a river close to a Canadian airport due to accidental release of fire-fighting foams (Moody *et al.* 2002). Furthermore, extremely high PFOS concentrations up to $1,650 \text{ mg L}^{-1}$ have been

measured in wastewater from a semiconductor manufacturing process (Tang *et al.* 2006).

Many attempts have been made to eliminate PFCs including PFOS and PFOA from water. The proposed removal technologies include activated sludge (Ochoa-Herrera & Sierra-Alvarez 2008; Zhou *et al.* 2010), anaerobic defluorination (Liou *et al.* 2010), adsorption (Ochoa-Herrera & Sierra-Alvarez 2008; Carter & Farrell 2010; Senevirathna *et al.* 2010; Chen *et al.* 2011), reverse osmosis (Tang *et al.* 2006), oxidation (Giri *et al.* 2011), reduction (Hori *et al.* 2006; Park *et al.* 2009), sonolysis (Moriwaki *et al.* 2005; Cheng *et al.* 2008; Vecitis *et al.* 2008), and incineration (Taylor *et al.* 2014). Several recent reviews of PFC treatment technologies (Vecitis *et al.* 2009; Yao *et al.* 2013) have shown that adsorption is a promising approach for removing PFCs from water. Reverse osmosis and sonolysis also appear to be viable methods, but these techniques are still in the development stage without any fully tested and sanctioned large-scale application. In terms of adsorptive technologies, some commercially available adsorbents (e.g., activated carbon, carbon nanotube (CNT), ion-exchange resin, and non-ion-exchange polymer (NEP)) and maize straw ash have been found to be capable of effectively adsorbing PFCs under certain conditions. This study aimed to evaluate the efficiencies of different commercially available adsorbents under the same test conditions. Granular activated carbon (GAC), powdered activated carbon (PAC), multi-walled carbon nanotube (MCN), double-walled carbon nanotube (DCN), anion-exchange resins (AERs), and NEP were selected as target adsorbents, because previous studies have shown that they were capable of removing PFOS and/or PFOA from aqueous solutions (Ochoa-Herrera & Sierra-Alvarez 2008; Deng *et al.* 2010; Senevirathna *et al.* 2010; Chen *et al.* 2011). These materials were previously investigated by different researchers under different test conditions; therefore, it is difficult to compare their efficiencies and determine the most effective adsorbent for PFOS and PFOA. For comparison purposes, alumina (ALU) (Wang & Shih 2011) and silica (SIL) (Tang *et al.* 2010) were also included in the tests. Possible strategies for future research and development are also discussed.

METHODS

Materials

High purity PFOS (97%) and PFOA (96%) neat standards were purchased from SynQuest Labs, Inc. (USA) and Sigma-Aldrich (Canada), respectively. They were used to prepare the stock and

working solutions for laboratory experiments. GAC (Filtrisorb 400) and PAC (WPL) were purchased from Brenntag Canada Inc. (Canada). CNTs (MCN and DCN), ALU (aluminum oxide, micron-sized), and SIL (silicon dioxide, nanopowder) were obtained from Sigma-Aldrich (Canada). AERs (IRA67 and IRA400) and NEP (Amb XAD4) were obtained from Octochem, Inc. (USA). A summary of physical properties of the adsorbents tested in this study is presented in the Supplementary Material, Table S1 (available online at <http://www.iwaponline.com/wst/070/445.pdf>). Polypropylene (PP) flasks, centrifuge tubes, and chromatography columns were purchased from General Laboratory Supply (USA), VWR International (Canada), and Evergreen Scientific (USA), respectively. Analytical standard solutions of PFOS, PFOA, ^{13}C -PFOS, and ^{13}C -PFOA were purchased from Wellington Laboratories (Canada). Solid phase extraction (SPE) cartridges (Oasis WAX) were purchased from Waters Corp. (USA). High performance liquid chromatography (HPLC)-grade methanol, acetonitrile, and water were obtained from Fisher Scientific (Canada).

Adsorption experiments

Kinetic and isotherm experiments

For adsorption kinetic experiments, three types of adsorbents, that is, GAC, MCN, and AER (IRA67), were tested separately at room temperature (21 °C). Weighed adsorbents (20 mg) were placed into 15 mL PP centrifuge tubes. After adding test solutions (10 mL) containing PFOS and PFOA (initial concentration: 50 mg L⁻¹ for each; pH 5), the tubes were immediately closed, placed horizontally on an orbital shaker, and shaken for a certain period of time at the speed of 300 rpm. Sampling was performed at time intervals of 0, 1, 2, 4, 24, 48, 72, and 96 h. No apparent pH changes were observed after the experiments.

Isotherm experiments were conducted for six adsorbents, that is, GAC, MCN, DCN, AER (IRA67), NEP, and ALU. PFOS/PFOA solutions (initial concentration: 10, 25, 50, 100, 200, 300, 400, and 500 mg L⁻¹ for each; pH 5) were added into 15 mL PP centrifuge tubes containing one specific adsorbent (10 mg). Then, the tubes were immediately closed, placed horizontally on an orbital shaker, and shaken for 96 h (300 rpm). Only minor changes in pH (within 1 log unit) were observed after the experiments.

PFC removal efficiency experiments

PFC removal efficiency experiments were performed for eight adsorbents, including GAC, PAC, MCN, AERs

(IRA67 and IRA400), NEP, ALU, and SIL. For each of these adsorbents, the same volume of material (5 mL) was placed into a 25 mL PP chromatography column. Then, a test solution (20 mL) containing PFOS and PFOA (50 mg L^{-1} for each) was added for filtration. The filtrates were collected in 50 mL PP centrifuge tubes.

Sample preparation

After shaking, all tubes were centrifuged at 3000 rpm for 20 min. An aliquot (5 mL) of the supernatant was taken from each tube for either analysis by direct injection or SPE preparation followed by instrumental analysis. All samples with a PFOS/PFOA concentration above $1 \mu\text{g L}^{-1}$ were directly analyzed by liquid chromatography–tandem mass spectrometry (LC/MS/MS). In this case, a $187.5 \mu\text{L}$ aliquot of sample was transferred to a PP culture tube. A volume of $125 \mu\text{L}$ of acetonitrile and $25 \mu\text{L}$ of isotopically labeled internal standard solution mixture were added to each sample aliquot. The samples were mixed and transferred to PP vials for analysis. For low concentration samples, a 4 mL aliquot of each sample was transferred to a 50 mL PP centrifuge tube. Forty-six millilitres of deionized water and $50 \mu\text{L}$ of isotopically labeled internal standard solution mixture were added to each sample aliquot. The pH was adjusted to 4–5 with a dilute formic acid solution. The SPE cartridge was conditioned with methanol followed by deionized water. Then, the entire sample was loaded onto the cartridge. The SPE cartridge was washed with 2 mL of 2% formic acid solution, followed by 4 mL of methanol. The cartridges were dried under vacuum for a minimum of 10 min. Samples were eluted with 2 mL of 1% ammonium hydroxide in methanol solution twice. The sample eluents were dried completely under nitrogen at approximately 45°C . The samples were reconstituted with a deionized water/acetonitrile (6:4) solution and then transferred to PP vials for analysis.

Sample analysis

The concentrations of PFOS and PFOA were analyzed by LC/MS/MS. A HPLC (Agilent 1100 Series)/Mass Spec (AB Sciex API 4000) system was used. Electrospray ionization operating in the negative ion mode was applied. A $15 \mu\text{L}$ aliquot of sample was injected into a Waters XBridge C18 column (ambient temperature) and gradient elution (mobile phase A: 20 mM ammonium acetate; mobile phase B: acetonitrile/methanol) was utilized. Multiple reaction monitoring transitions for PFOS and PFOA were

499–80 and 413–369 m/z , respectively. The PFOS and PFOA concentrations were quantified using standard calibration curves established with internal standards. The reporting detection limits for both PFOS and PFOA were 0.001 mg L^{-1} .

Quality assurance/quality control

PP equipment was used in the experiments according to previous studies (Becker *et al.* 2008; Chen *et al.* 2011) and Teflon equipment was avoided (Becker *et al.* 2008). Quality control samples, including standard solutions and duplicate samples, were prepared and analyzed with the test samples under the same conditions. Sample analysis was performed at Maxxam Analytics (Mississauga, ON, Canada). Maxxam is accredited by the Standard Council of Canada for PFC analysis in environmental matrices. All laboratory operations were monitored using strict quality assurance/quality control measures. These included a laboratory blank, blank spike, and matrix spike for each sample batch. A multi-point calibration curve was analyzed with each analytical sequence during LC/MS/MS analysis. For PFOS, the measured average blank spike recovery was 104% (standard deviation (SD) = 6%, $n = 7$) and matrix spike recovery was 104% ($n = 1$). For PFOA, the average blank spike recovery was 99% (SD = 14%, $n = 7$) and matrix spike recovery was 104% ($n = 1$). PFOS and PFOA were not detected in the method blanks; thus no recovery or blank correction was applied to the analytical results.

RESULTS AND DISCUSSION

Adsorption kinetics

In order to assess the influence of contact time on PFC removal by different adsorbents, several kinetic tests were performed. Three adsorbents, GAC, MCN, and AER (IRA67), were selected as the target materials based on our previous literature review (Yao *et al.* 2013). An initial concentration (C_0) of 50 mg L^{-1} was used for both PFOS and PFOA. Currently, only limited information is available regarding PFC concentrations in contaminated groundwater (0.13 – 7.1 mg L^{-1}) (Moody & Field 1999). Moody *et al.* (2002) reported that the total perfluorinated surfactant concentration in surface water samples ranged from <0.01 to 17 mg L^{-1} , following an accidental release of fire-fighting foam into Etobicoke Creek, ON, Canada, in June 2000. In addition, an extremely high PFOS concentration up to

1,650 mg L⁻¹ was reported in a semiconductor wastewater (Tang *et al.* 2006).

Figure 1 shows the kinetic profiles of the three adsorbents. For both PFOS and PFOA, the adsorption equilibrium to AER (IRA67), a polyacrylic resin, was reached within 2 h of contact. The time required to reach equilibrium for PFOS and PFOA onto MCN was approximately 2 and 4 h, respectively. For GAC, the equilibrium was reached within 24 h for PFOS and PFOA. Previously, Deng *et al.* (2010) reported that about 48 h was required to reach the adsorption equilibrium for AER (IRA67), while 168 h was needed for polystyrene resins (i.e., IRA400, IRA410, IRA96, and IRA900) ($C_0 = 200$ mg L⁻¹). For CNTs, Chen *et al.* (2011) found that PFOS adsorption equilibrium could be reached within 2 h ($C_0 = 100$ mg L⁻¹). For GAC (Filtrisorb 400), Yu *et al.* (2009) observed very slow adsorption kinetics for both PFOS and PFOA (≥ 168 h) ($C_0 = 50$ mg L⁻¹ for each), while Senevirathna *et al.* (2010) reported an equilibrium time of 4 h for PFOS ($C_0 = 5$ mg L⁻¹).

The observed difference in equilibrium time among the adsorbents suggested different adsorption mechanisms. The shortest equilibrium time for AER (IRA67) might be due to the electrostatic attraction between negatively charged PFOS/PFOA and AER, which accelerates the

adsorption rate. The shorter equilibrium time for MCN compared to GAC is likely related to its high available space for adsorption that exists on the cylindrical external surface. GAC has much more micropore area and less meso-/macropore area than MCN, thus causing longer time for PFC molecules to diffuse into the micropores of GAC to reach equilibrium.

To further understand the adsorption kinetics, the pseudo-second-order (PSO) model was applied to fit the kinetic data (Senevirathna *et al.* 2010; Chen *et al.* 2011). The PSO model is expressed by Equation (1) as follows:

$$\frac{dq_t}{dt} = k(q_e - q_t)^2 \quad (1)$$

where q_e and q_t are the amount of PFC adsorbed onto the adsorbent at equilibrium and at time t (mg g⁻¹), respectively, and k is the rate constant (g mg⁻¹ h⁻¹). Equation (1) can be arranged to give Equation (2).

$$\frac{t}{q_t} = \frac{t}{q_e} + \frac{1}{kq_e^2} = \frac{t}{q_e} + \frac{1}{v_0} \quad (2)$$

where v_0 is the initial adsorption rate (mg g⁻¹ h⁻¹). Equation (2) can be plotted as t/q_t vs. t . A linear dependency

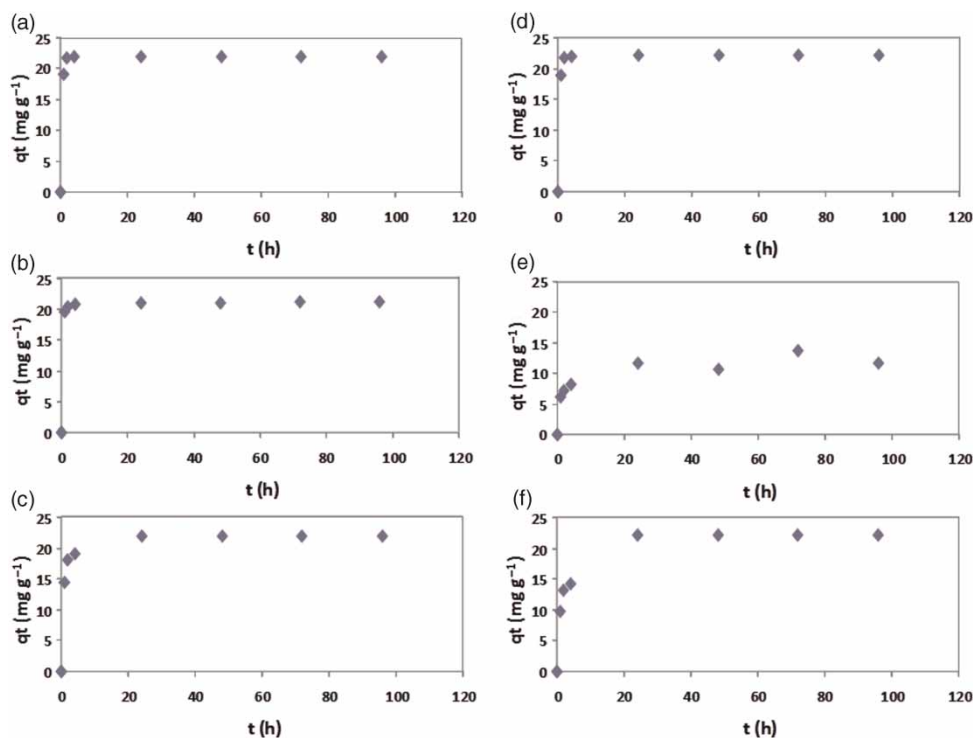


Figure 1 | Adsorption kinetics of PFOS onto (a) AER (IRA67), (b) MCN, and (c) GAC; and PFOA onto (d) AER (IRA67), (e) MCN, and (f) GAC.

would suggest a good fit between the experimental results and the model. This model assumes that the adsorption rate is controlled by chemical adsorption and the adsorption capacity is proportional to the number of active sites occupied on the adsorbent (Ho & McKay 1999).

It was found that the PSO model fits all the adsorption data well as indicated by the high R^2 values (0.99–1.00) shown in Table 1, suggesting the dominance of chemical adsorption in the adsorption processes. The initial adsorption rates (v_0 , $\text{mg g}^{-1} \text{h}^{-1}$) of PFOS and PFOA onto the adsorbents varied in an order of AER ($385 \text{ mg g}^{-1} \text{h}^{-1}$) > MCN ($175 \text{ mg g}^{-1} \text{h}^{-1}$) > GAC ($51.0 \text{ mg g}^{-1} \text{h}^{-1}$), and AER ($313 \text{ mg g}^{-1} \text{h}^{-1}$) > GAC ($16.2 \text{ mg g}^{-1} \text{h}^{-1}$) > MCN ($7.6 \text{ mg g}^{-1} \text{h}^{-1}$), respectively. These results indicated that the PFC adsorption onto AER has a much higher initial rate compared to GAC and MCN. Meanwhile, the comparison of measured q_e values from different adsorbents showed that the quantities of PFOS and PFOA adsorbed by AER (22.0 and 22.2 mg g^{-1}) and GAC (22.1 and 22.7 mg g^{-1}) at equilibrium were almost the same, but greater than those adsorbed by MCN (21.3 and 12.4 mg g^{-1}).

The adsorption process on porous adsorbents could involve diffusion mechanisms, such as intra-particle diffusion (IPD), external diffusion, and boundary layer diffusion. The IPD model was used to determine whether IPD plays an important role, particularly for MCN and GAC. IPD was expected to be negligible for AER due to its low porosity. The model is defined as Equation (3) as follows:

$$q_t = k_p t^{1/2} \quad (3)$$

where k_p ($\text{mg g}^{-1} \text{h}^{-1/2}$) is the IPD rate constant.

Table 1 | Kinetic parameters of the PSO and IPD models for PFOS and PFOA on AER (IRA67), MCN, and GAC

Adsorbent	PSO model			IPD model		
	q_e (mg g^{-1})	v_0 ($\text{mg g}^{-1} \text{h}^{-1}$)	k ($\text{g mg}^{-1} \text{h}^{-1}$)	R^2	Intercept	R^2
<i>PFOS</i>						
AER	22.0	385	0.793	1.00	3.02	0.46
MCN	21.3	175	0.388	1.00	3.00	0.79
GAC	22.1	51.0	0.104	1.00	2.78	0.83
<i>PFOA</i>						
AER	22.2	313	0.633	1.00	3.01	0.48
MCN	12.4	7.6	0.049	0.99	1.88	0.92
GAC	22.7	16.2	0.032	1.00	2.39	0.93

Equation (3) can also be linearized with respect to time t to produce Equation (4) as follows:

$$\ln q_t = \ln k_p + \frac{1}{2} \ln t \quad (4)$$

Linear dependency of $\ln q_t$ vs. $\ln t$ would suggest a good fit with the IPD model. This model assumes that the external diffusion and boundary layer diffusion are negligible and the IPD is the only rate-controlling mechanism. If the regression of $\ln q_t$ vs. $\ln t$ is linear and passes through the origin, then the IPD is the sole rate-controlling step.

The IPD calculation showed that the regression for PFOS adsorption on MCN and GAC was nonlinear, with low R^2 values (0.79 and 0.83) and positive intercepts (Table 1). In terms of PFOA, the regression was linear with R^2 values of 0.92 and 0.93, but the plots had positive intercepts. All of these suggested that the IPD was not the only adsorption rate-controlling mechanism for MCN and GAC. For AER (IRA67), as expected, the calculated R^2 values for PFOS and PFOA were only 0.46 and 0.48, respectively, indicating that IPD was not an important mechanism (Table 1).

Adsorption isotherms

Six adsorbents were tested to investigate their adsorption isotherms. These were GAC, MCN, DCN, AER (IRA67), NEP, and ALU. According to the literature review (Yao et al. 2013) and the kinetic experiments conducted in the study, the contact time for isotherm experiments was set to be 96 h, which ensures that all adsorption processes have reached their equilibrium during the duration. The initial PFOS and PFOA concentration range (10 – 500 mg L^{-1}) used in this study could cover the potential aqueous streams such as AFFF-impacted groundwater and surface water (Moody et al. 2002), as well as PFC-contaminated industrial wastewater (Tang et al. 2006). The adsorption capacities of the tested adsorbents were estimated by fitting the experimental data to the Freundlich model. The Freundlich equation is an empirical relationship describing the adsorption of solutes from a liquid to a solid surface. It has been widely used to describe adsorption processes for PFCs onto heterogeneous surfaces, including activated carbon (Senevirathna et al. 2010), CNTs (Chen et al. 2011), ion-exchange polymers (Deng et al. 2010; Senevirathna et al. 2010), NEPs (Senevirathna et al. 2010), and ALU (Wang & Shih 2011) in aqueous solutions.

The Freundlich model is defined as Equation (5) as follows:

$$q_e = K_F C_e^n \quad (5)$$

where q_e (mg g^{-1}) is the equilibrium concentration in the solid phase, C_e (mg L^{-1}) is the equilibrium concentration of solute in solution, K_F ($\text{mg}^{(1-n)} \text{L}^n \text{g}^{-1}$) is the Freundlich adsorption constant or capacity factor and n is the Freundlich exponent. According to this equation, adsorption capacity of a given adsorbent is proportional to the equilibrium concentration of the given adsorbate. Equation (5) can also be rearranged into linear format as Equation (6).

$$\log q_e = \log K_F + n \log C_e \quad (6)$$

A linear dependency would suggest a good fit between the experimental results and the model.

Since the observed adsorption isotherms of PFOS and PFOA onto the tested adsorbents in this study generally fit well with the Freundlich model (see Figures S1 and S2 of the Supplementary Material, available online at <http://www.iwaponline.com/wst/070/445.pdf>), the adsorption capacities of these materials were calculated based on the model, and the results are shown in Table 2.

Adsorption of PFOS

As can be seen in Table 2, under our test conditions, the adsorption capacities of the investigated adsorbents varied

Table 2 | Calculated equilibrium parameters using the Freundlich model for PFOS and PFOA adsorption on different adsorbents

	K_F ($\text{mg}^{(1-n)} \text{L}^n \text{g}^{-1}$)	n	R^2
<i>PFOS</i>			
AER	7,300	0.90	0.73
GAC	120	0.29	0.95
DCN	82	0.31	0.97
MCN	34	0.40	0.99
NEP	7.3	0.68	0.98
ALU	0.6	1.03	1.00
<i>PFOA</i>			
AER	200	0.97	0.92
GAC	63	0.35	0.93
DCN	35	0.34	0.98
MCN	5.4	0.78	0.95
NEP	0.9	1.27	0.95
ALU	0.7	1.39	0.89

in the order of AER (IRA67) > GAC > DCN > MCN > NEP > ALU. The AER (IRA67) exhibited a highly enhanced adsorption capacity coefficient constant (K_F) for PFOS ($7,300 \text{ mg}^{(1-n)} \text{L}^n \text{g}^{-1}$), indicating that IRA67 is the best material for PFOS removal among the tested adsorbents. GAC also showed a high K_F value of $120 \text{ mg}^{(1-n)} \text{L}^n \text{g}^{-1}$, which is in line with previously reported values. For example, Ochoa-Herrera & Sierra-Alvarez (2008) and Yu *et al.* (2009) estimated the K_F value as 61 and $215 \text{ mg}^{(1-n)} \text{L}^n \text{g}^{-1}$, respectively. In terms of CNTs, DCN was found to have higher adsorption capacity ($82 \text{ mg}^{(1-n)} \text{L}^n \text{g}^{-1}$) compared to MCN ($34 \text{ mg}^{(1-n)} \text{L}^n \text{g}^{-1}$). Previously, Chen *et al.* (2011) observed that the adsorption capacities of CNTs decreased in the order: single-walled carbon nanotube (SCN) ($122 \text{ mg}^{(1-n)} \text{L}^n \text{g}^{-1}$) > MCN10 ($47.1 \text{ mg}^{(1-n)} \text{L}^n \text{g}^{-1}$) > MCN50 ($14.9 \text{ mg}^{(1-n)} \text{L}^n \text{g}^{-1}$), which is in line with the decrease in their BET surface area (SCN: $547 \text{ m}^2 \text{g}^{-1}$; MCN10: $325 \text{ m}^2 \text{g}^{-1}$; MCN50: $97 \text{ m}^2 \text{g}^{-1}$) (Chen *et al.* 2011). In addition, ALU showed very low K_F values ($<1 \text{ mg}^{(1-n)} \text{L}^n \text{g}^{-1}$).

The calculated low R^2 value (0.73) for AER (IRA67) (Table 2) is likely due to the presence of different stages in the isotherm of PFOS on the adsorbent, namely a very steep isotherm at lower concentration level (when $C_0 \leq 100 \text{ mg L}^{-1}$; see the dashed line shown in Figure S1(a)) and a less steep one within higher concentration range ($100 \text{ mg L}^{-1} \leq C_0 \leq 500 \text{ mg L}^{-1}$; see the dash-dot line shown in Figure S1(a)). Our preliminary isotherm tests conducted with a C_0 between 0.05 and 50 mg L^{-1} indicated steeper slopes and higher K_F values for both of the PFCs on AER (IRA67) and GAC. Similar phenomena were reported by Carter & Farrell (2010). They observed two changes in slope for the PFOS and PFBS isotherms on GAC in ultrapure water. The obtained n values for all the adsorbents, except AER and ALU, were not close to 1, ranging from 0.29 to 0.68 (Table 2). This might be related to adsorption site heterogeneity and/or adsorbate-adsorbent interactions such as the electrostatic repulsion since high concentrations of PFOS and PFOA were used (Yu *et al.* 2009). Chen *et al.* (2011) previously investigated the adsorption isotherms of PFOS by chars, ash, and CNTs ($C_0 = 100 \text{ mg L}^{-1}$) and found that all isotherms were nonlinear, with n values ranging from 0.32 to 0.57. They considered that the nonlinearity was largely attributed to the electrostatic repulsion between the adsorbed and freely dissolved PFOS ions.

Adsorption of PFOA

For PFOA adsorption, the observed K_F values ($\text{mg}^{(1-n)} \text{L}^n \text{g}^{-1}$) varied in the same order: AER (IRA67) (200) > GAC

(63) > DCN (35) > MCN (5.4) > NEP (0.9) > ALU (0.7) (Table 2), indicating that AER (IRA67) has the highest capacity to remove PFOA from water at mg L^{-1} level. The K_F values reported by Ochoa-Herrera & Sierra-Alvarez (2008) and Yu *et al.* (2009) are 12 and $195 \text{ mg}^{(1-n)} \text{ L}^n \text{ g}^{-1}$, respectively.

It is worthy to note that all tested adsorbents, except ALU, showed higher adsorption capacities for PFOS compared to those for PFOA. Since there is very little information currently available on PFOA adsorption, the new data generated from this study provided important information for selecting proper materials to effectively remove specific PFC molecules from water.

PFC removal efficiency

Tests were conducted to confirm and compare the PFOS/PFOA removal efficiencies by different materials. The results are shown in Figure 2. For PFOS, the removal efficiencies of the tested adsorbents varied in the order of MCN (100%) ~ AER (IRA67) (100%) > GAC (99%) > AER (IRA400) (96%) > NEP (71%) > ALU (56%). Similar results were obtained for PFOA removal: MCN (100%) > AER

(IRA400) (99%) ~ AER (IRA67) (99%) > GAC (98%) > NEP (40%) > ALU (24%). These results indicated that MCN and AER (IRA67) have highest PFOS/PFOA removal efficiencies (>99%) among the tested adsorbents. This might be attributed to their short equilibrium times (i.e., 2–4 h) as discussed above. GAC showed comparable removal efficiency (99%) for PFOS, but a bit less efficiency (98%) for PFOA in the filtration tests, which might be due to its relatively longer equilibrium times for PFOS and PFOA. On the other hand, NEP and ALU showed poor removal efficiencies, indicating that these materials are not suitable for removing PFCs from water. In terms of PAC and SIL, although only trace levels of PFOS/PFOA were detected in the filtrates collected in their filtration experiments, these two materials were found to very easily clog the chromatography columns, making them unsuitable for practical application.

Considering the fact that (1) adsorption of both PFOS and PFOA onto AER (IRA67) requires the shortest time to reach equilibrium (<2 h), (2) AER (IRA67) has highest K_F values for PFOS and PFOA, (3) AER (IRA67) possesses high removal efficiencies ($\geq 99\%$) for both PFOS and PFOA, (4) GAC has second highest K_F values for PFOS

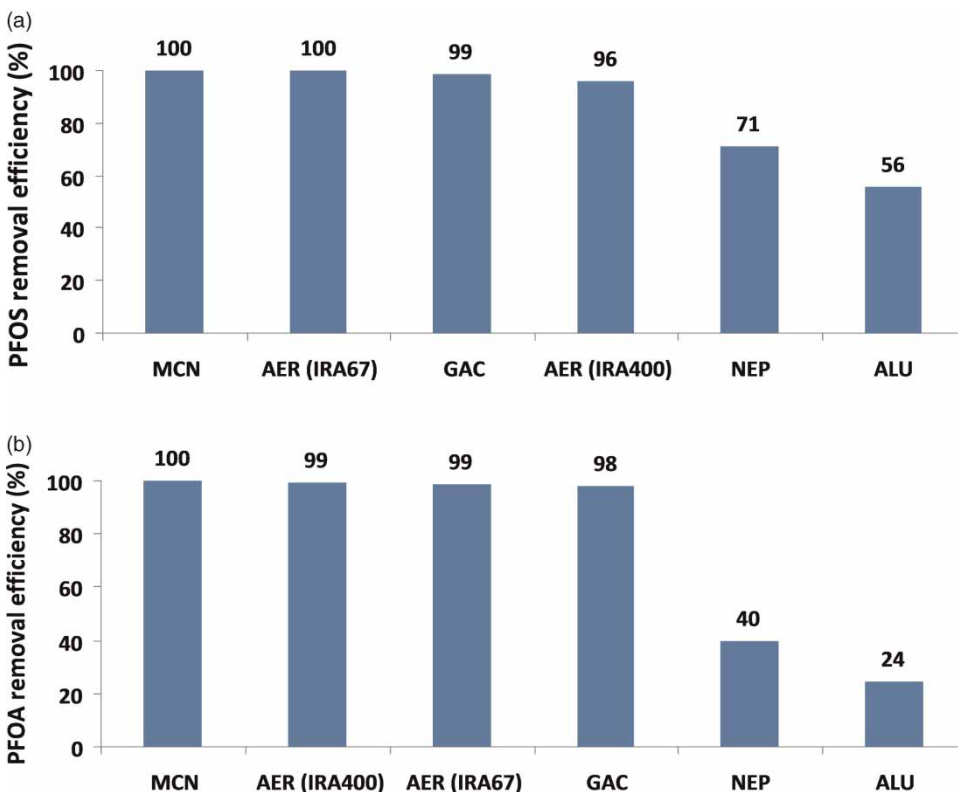


Figure 2 | Removal efficiencies (%) by different adsorbents for (a) PFOS and (b) PFOA.

and PFOA, (5) GAC possesses high removal efficiencies for PFOS (99%) and PFOA (98%), and (6) AER (IRA67) and GAC are much more cost effective compared to CNTs, AER (IRA67) was identified as the most promising adsorption material for the removal of PFOS and PFOA from PFC-contaminated water at mg L⁻¹ level, and GAC could also be a preferred adsorbent.

CONCLUSIONS

This study demonstrated that adsorption is an effective technique for the removal of PFCs, such as PFOS and PFOA, from aqueous solutions. The experimental results suggested that two adsorbents, AER (IRA67) and GAC (Filtrisorb 400), have overall superior characteristics (i.e., high adsorption capacity, short equilibrium time, easy to use, and relatively low cost) compared to other commercially available candidate adsorbents tested in the study. In order to identify the most effective adsorbent that can be practically used for the groundwater treatment at PFC-contaminated sites, further investigations are needed to evaluate their PFC removal capacities with actual contaminated groundwater and other co-occurring pollutants such as hydrocarbons and other AFFF components.

ACKNOWLEDGMENTS

This study was funded by Environment Canada's Compliance Promotion and Contaminated Sites Division (CPCSD) under the Federal Contaminated Sites Action Plan (FCSAP) program. We are grateful to Kathy Kitagawa and Jeremy Anglesey of CPCSD for valuable discussions and organizational support.

REFERENCES

- Becker, A. M., Gerstmann, S. & Frank, H. 2008 Perfluorooctane surfactants in waste waters, the major source of river pollution. *Chemosphere* **72**, 115–121.
- Carter, K. E. & Farrell, J. 2010 Removal of perfluorooctane and perfluorobutane sulfonate from water via carbon adsorption and ion exchange. *Sep. Sci. Technol.* **45**, 762–767.
- Chen, X., Xia, X., Wang, X., Qiao, J. & Chen, H. 2011 A comparative study on sorption of perfluorooctane sulfonate (PFOS) by chars, ash and carbon nanotubes. *Chemosphere* **83**, 1313–1319.
- Cheng, J., Vecitis, C. D., Park, H., Mader, B. T. & Hoffmann, M. R. 2008 Sonochemical degradation of perfluorooctane sulfonate (PFOS) and perfluorooctanoate (PFOA) in landfill groundwater: environmental matrix effects. *Environ. Sci. Technol.* **42**, 8057–8063.
- Deng, S., Yu, Q., Huang, J. & Yu, G. 2010 Removal of perfluorooctane sulfonate from wastewater by anion exchange resins: effects of resin properties and solution chemistry. *Water Res.* **44**, 5188–5195.
- Fujii, S., Tanaka, S., Lien, N. P. H., Qiu, Y. & Polprasert, C. 2007 New POPs in the water environment: distribution, bioaccumulation and treatment of perfluorinated compounds – a review paper. *J. Water Supply Res. Technol. AQUA* **56**, 313–326.
- Giri, R. R., Ozaki, H., Morigaki, T., Taniguchi, S. & Takanami, R. 2011 UV photolysis of perfluorooctanoic acid (PFOA) in dilute aqueous solution. *Water Sci. Technol.* **63**, 276–282.
- Hansen, K. J., Johnson, H. O., Eldridge, J. S., Butenhoff, J. L. & Dick, L. A. 2002 Quantitative characterization of trace levels of PFOS and PFOA in the Tennessee River. *Environ. Sci. Technol.* **36**, 1681–1685.
- Ho, Y. S. & McKay, G. 1999 Pseudo-second order model for sorption processes. *Process Biochem.* **34**, 451–465.
- Hori, H., Nagaoka, Y., Yamamoto, A., Sano, T., Yamashita, N., Taniyasu, S., Kutsuna, S., Osaka, I. & Arakawa, R. 2006 Efficient decomposition of environmentally persistent perfluorooctanesulfonate and related fluorochemicals using zerovalent iron in subcritical water. *Environ. Sci. Technol.* **40**, 1049–1054.
- Lien, N. P. H., Fujii, S., Tanaka, S., Nozoe, M. & Tanaka, H. 2008 Contamination of perfluorooctane sulfonate (PFOS) and perfluorooctanoate (PFOA) in surface water of the Yodo River basin (Japan). *Desalination* **226**, 338–347.
- Liou, J. S., Szostek, B., DeRito, C. M. & Madsen, E. L. 2010 Investigating the biodegradability of perfluorooctanoic acid. *Chemosphere* **80**, 176–183.
- Moody, C. A. & Field, J. A. 1999 Determination of perfluorocarboxylates in groundwater impacted by fire-fighting activity. *Environ. Sci. Technol.* **33**, 2800–2806.
- Moody, C. A., Martin, J. W., Kwan, W. C., Muir, D. C. G. & Mabury, S. A. 2002 Monitoring perfluorinated surfactants in biota and surface water samples following an accidental release of fire-fighting foam into Etobicoke Creek. *Environ. Sci. Technol.* **36**, 545–551.
- Moriwaki, H., Takagi, Y., Tanaka, M., Tsuruho, K., Okitsu, K. & Maeda, Y. 2005 Sonochemical decomposition of perfluorooctane sulfonate and perfluorooctanoic acid. *Environ. Sci. Technol.* **39**, 3388–3392.
- Murakami, M., Shinohara, H. & Takada, H. 2009 Evaluation of wastewater and street runoff as sources of perfluorinated surfactants (PFSS). *Chemosphere* **74**, 487–495.
- Ochoa-Herrera, V. & Sierra-Alvarez, R. 2008 Removal of perfluorinated surfactants by sorption onto granular activated carbon, zeolite and sludge. *Chemosphere* **72**, 1588–1593.
- Park, H., Vecitis, C. D., Cheng, J., Choi, W., Mader, B. T. & Hoffmann, M. R. 2009 Reductive defluorination of aqueous

- perfluorinated alkyl surfactants: effects of ionic headgroup and chain length. *J. Phys. Chem. A* **113**, 690–696.
- Schultz, M. M., Barofsky, D. F. & Field, J. A. 2004 Quantitative determination of fluorotelomer sulfonates in groundwater by LC MS/MS. *Environ. Sci. Technol.* **38**, 1828–1835.
- Senevirathna, S. T. M. L. D., Tanaka, S., Fujii, S., Kunacheva, C., Harada, H., Shivakoti, B. R. & Okamoto, R. 2010 A comparative study of adsorption of perfluorooctane sulfonate (PFOS) onto granular activated carbon, ion-exchange polymers and non-ion-exchange polymers. *Chemosphere* **80**, 647–651.
- So, M. K., Taniyasu, S., Yamashita, N., Giesy, J. P., Zheng, J., Fang, Z., Im, S. H. & Lam, P. K. S. 2004 Perfluorinated compounds in coastal waters of Hong Kong, South China, and Korea. *Environ. Sci. Technol.* **38**, 4056–4063.
- Tang, C. Y., Fu, Q. S., Robertson, A. P., Criddle, C. S. & Leckie, J. O. 2006 Use of reverse osmosis membranes to remove perfluorooctane sulfonate (PFOS) from semiconductor wastewater. *Environ. Sci. Technol.* **40**, 7343–7349.
- Tang, C. Y., Fu, Q. S., Gao, D., Criddle, C. S. & Leckie, J. O. 2010 Effect of solution chemistry on the adsorption of perfluorooctane sulfonate onto mineral surfaces. *Water Res.* **44**, 2654–2662.
- Taylor, P. H., Yamada, T., Striebich, R. C., Graham, J. L. & Giraud, R. J. 2014 Investigation of waste incineration of fluorotelomer-based polymers as a potential source of PFOA in the environment. *Chemosphere* **110**, 17–22.
- Vecitis, C. D., Park, H., Cheng, J., Mader, B. T. & Hoffmann, M. R. 2008 Kinetics and mechanism of the sonolytic conversion of the aqueous perfluorinated surfactants, perfluorooctanoate (PFOA), and perfluorooctane sulfonate (PFOS) into inorganic products. *J. Phys. Chem. A* **112**, 4261–4270.
- Vecitis, C. D., Park, H., Cheng, J., Mader, B. T. & Hoffmann, M. R. 2009 Treatment technologies for aqueous perfluorooctanesulfonate (PFOS) and perfluorooctanoate (PFOA). *Front. Environ. Sci. Eng. China* **3**, 129–151.
- Wang, F. & Shih, K. 2011 Adsorption of perfluorooctanesulfonate (PFOS) and perfluorooctanoate (PFOA) on alumina: influence of solution pH and cations. *Water Res.* **45**, 2925–2930.
- Yao, Y., Volchek, K., Brown, C. E., Lambert, P., Gamble, L., Kitagawa, K., Anglesey, J., Dugas, A., Punt, M. & Velicogna, D. 2013 Remedial options for PFC contaminated sites: a review. In: *Proceedings of the 36th AMOP Technical Seminar on Environmental Contamination and Response*. Environment Canada, Ottawa, ON, Canada, pp. 654–672.
- Yu, Q., Zhang, R., Deng, S., Huang, J. & Yu, G. 2009 Sorption of perfluorooctane sulfonate and perfluorooctanoate on activated carbons and resin: kinetic and isotherm study. *Water Res.* **43**, 1150–1158.
- Zhou, Q., Deng, S. B., Zhang, Q. Y., Fan, Q., Huang, J. & Yu, G. 2010 Sorption of perfluorooctane sulfonate and perfluorooctanoate on activated sludge. *Chemosphere* **81**, 453–458.

First received 24 April 2014; accepted in revised form 27 October 2014. Available online 8 November 2014